Design and Implementation of a Cuk Converter Controlled by a Direct Duty Cycle INC-MPPT in PV Battery System

Abdelhakim BELKAID[a,b], Ilhami COLAK[c,*], Korhan KAYISLI[c], Ramazan BAYINDIR[d]

belkaid08@yahoo.fr; ilhcol@gmail.com; korhankayisli@gmail.com; bayindir@gazi.edu.tr

[a]*Department of Electromechanics, University of Bordj Bou Arreridj, El-Anasser 34030, Bordj Bou Arreridj, Algeria*
[b]*Automatic Laboratory of Setif (LAS), University of Setif 1, El Maabouda, Street of Bejaia, 19000 Setif, Algeria*
[c]*Engineering and Architecture Faculty of Nisantasi University, Istanbul , Turkey*
[d]*Department of Electrical & Electronics Engineering, Gazi University, Faculty of Technology, 06500, Turkey*

Received: 26.12.2018 Accepted:12.03.2019

***Abstract*—The performance of a solar energy system can be better by inserting a smart power converter with an appropriate MPPT control between the PV source and the load. The smart converter or the well-known as PCU is employed to maximize the power extracted from the solar panel by real-time impedance matching, and to regulate the PV voltage level. The proposed PCU is equipped with a cuk DC-DC converter controlled by a smart energy recovery technique based on direct duty cycle INC algorithm. The review and validity of the proposed PCU model, which interfaces an MSX 60 module with a 12V lead-acid battery, was performed using the Matlab tools. The designed system works effectively and provides the best performance in transient and stable states, regardless of variations in environmental conditions.**

***Index Terms*—PV systems; Cuk DC-DC converter; Lead–acid battery; direct duty cycle INC-MPPT; power conditioning unit.**

NOMENCLATURE

P_{max}	Maximum power
V_{oc}	Open-circuit voltage
I_{sc}	Short-circuit current
V_{mpp}	Voltage at MPP
I_{mpp}	Current at MPP
k_v	Temperature coefficient of V_{oc}
k_i	Temperature coefficient of I_{sc}
f	Switching frequency
$L_1 \& L_2$	Inductors
$C_1 \& C_2$	Capacitors
R	Resistance
V_b	Battery nominal voltage
T_s	switching period
d	Duty cycle
u	switch position
V_{in}	Input voltage
V_{out}	Output voltage
INC	incremental conductance
MPP	maximum power point
MPPT	maximum power point tracking
PCU	power conditioning unit
PI	proportional–integral
SEPIC	Single ended primary inductor converter

I. INTRODUCTION

Everyone needs energy to live especially in this last century where people have an elevated standard of living. Electric energy is used by man for his daily needs such as: heating, illumination, cookery, distraction, information and communication, et cetera. In the 20th century, fossil fuels in their different forms of matter, coal, oil and natural gas, were widely used in power generation, resulting in huge carbon dioxide emissions. Environmental pollution, climate change, nuclear dangers, limitation of reserves of fossil resources and uranium, population enlargement and augmented energy demand, have made us conscious that the search for alternative energy alternatives to our planet is vital. Renewable energies such as photovoltaic can be a good solution, but they have a low yield and a high initial price [1].

The solar panel works unlike a lamp, it converts sunlight into electricity via the photovoltaic effect. The use of photovoltaic energy has never stopped growing. Solar energy is inexhaustible, non-polluting, modular and multidisciplinary involving electronics, mechanics, power electronics, command theory, etc. In PV systems, real-time impedance matching is possible using a power electronics interface that attaches the solar source with the charge. This task makes possible the optimal operating of the renewable source and thus the efficiency of the overall system will be great. Several types of DC/DC power converters can be utilized: voltage-raising structures, voltage-lowering structures, or both. In literature, we can find buck structure that acts as a step-down voltage [2], boost as a voltage step-up [1, 3], buck-boost structure [4], cuk configuration [5-6], zeta topology [7] or SEPIC converter [8-9] can play both roles, other structures with galvanic isolation like flyback [10] or forward [11] can be used also. The choice of one structure among others depends on various factors such as polarity and voltage gain. It can be seen that the polarity of

the static gain of the SEPIC and zeta structures is positive, while that of the cuk and buck-boost structures is negative.

To achieve impedance matching, the DC-DC converter must be controlled by a high performance MPPT algorithm. A great number of original MPPT algorithms have been used, such as: Perturbing and observing algorithm, Incremental Conductance, fractional open and short circuit techniques, neural network, sliding mode, fuzzy logic, etc. Various researchers have proposed modifications to these techniques to increase their efficacy.

In this work, an intelligent maximum power tracker consisting on a cuk-type converter, in which the command is based on a direct duty ratio INC algorithm with no using PI regulator, is investigated. The cuk circuit can be considered as an appropriate converter to exploit in the conception of the MPPT system because it presents weak losses and high yield [6]. The type of lead-acid storage battery was used because its structure is simple and its manufacturing price is low [12].

II. COMPARISON OF DC-DC POWER CONVERTERS

The impedance matching stage can take the different structures of the DC-DC converters. These vary according to: arrangement complication, selling cost, effectiveness, number of passive electronic components, current ripple at their entry and exit, tracking and non-tracking regions, static gain polarity and value, resistance adaptation rate, etc [13]. A diode, a switch that can be controlled and some passive electronic components for filtering make up the majority of power converters. The operating principle of these converters accepts two modes that depend on the position of the controllable switch. Each configuration has its own benefits and drawbacks. All converter configurations present a non linear duty cycle-voltage relation, except for the buck. In photovoltaic applications, to increase the life of the solar panels, the diodes are placed in series in order to prevent the flow of currents in the opposite direction, that is to say from the battery to the panel during unfavorable conditions like the night for example. An additional anti-return diode is essential for the buck, the boost, the cuk and the zeta converters, but the other two boost and SEPIC topologies do not need to add back-off diodes. The buck-boost, the cuk, the zeta and the SEPIC topologies can track the MPP over the entire current-voltage curve while the boost and the buck tracking region is restricted to a little zone in the 1st quadrant, which unnecessarily affects MPP monitoring. Boost topology is the most utilized converter for solar devices, but it does not effectively track the MPP in low light conditions. The preferred DC-DC converter may not meet all the conditions cited above; a compromise must be sought in the selection of the converter to be used in the photovoltaic system. A power converter that can be chosen for PV systems must fulfill the following conditions: operate simultaneously as a step-down and step-up voltage; follow the MPP over the entire current-voltage curve; provide uninterrupted input/output power flow with fewer ripples on the quantities of the output voltage, output current, and input current. Based on the previous comparative study, the convenient converter for the pursuit of the MPP can take one of the next four structures: SEPIC, cuk circuit, the buck-boost and zeta. For our study, we choose a cuk DC-DC converter controlled by direct duty cycle INC-MPPT.

III. MODELLING AND DESIGN OF THE CUK CIRCUIT

High efficiency, low switching losses and a smaller amount ripple in output current due to the output stage inductance make the cuk converter more attractive. The chopper circuit selected, its current waveforms, and its voltage waveforms are illustrated in Fig.1. Depending on the switch position, the proposed converter has two modes of operation. The first operating mode is realized by closing the switch (ON state). In this mode, the capacitance releases energy to the output. The ON mode is characterized by a set of equations:

$$\begin{aligned}\frac{di_L}{dt} &= \frac{V_{in}}{L_1}\\ \frac{dv_{c'}}{dt} &= \frac{i_{L'}}{C_1}\\ \frac{di_{L'}}{dt} &= \frac{V_{out}}{L_2} - \frac{V_{c'}}{L_2}\end{aligned} \quad (1)$$

The second operating mode is achieved by opening the switch (OFF state), the diode is forward biased and transfers the power to the charge. Capacitance C_1 charges from the PV source. The Off mode is characterized by equations (2):

$$\begin{aligned}\frac{di_L}{dt} &= \frac{V_{in}}{L_1} - \frac{V_{C'}}{L_1}\\ \frac{dv_{c'}}{dt} &= \frac{i_{L_1}}{C_1}\\ \frac{di_{L'}}{dt} &= \frac{V_{out}}{L_2}\end{aligned} \quad (2)$$

Dynamic equations of the cuk converter can be obtained by combining (1) and (2):

$$\begin{aligned}\frac{di_L}{dt} &= \frac{V_{in}}{L_1} - \frac{V_{C'}}{L_1}\cdot(1-u)\\ \frac{dv_{c'}}{dt} &= \frac{i_{L_1}}{C_1}\cdot(1-u) + \frac{i_{L'}}{C_1}\cdot u\\ \frac{di_{L'}}{dt} &= \frac{V_{out}}{L_2} - \frac{V_{c'}}{L_2}\cdot u\end{aligned} \quad (3)$$

The expressions (1) are applicable for the interval [0 to dT_s] and the expressions (2) are applicable for the interval [dT_s to T_s].

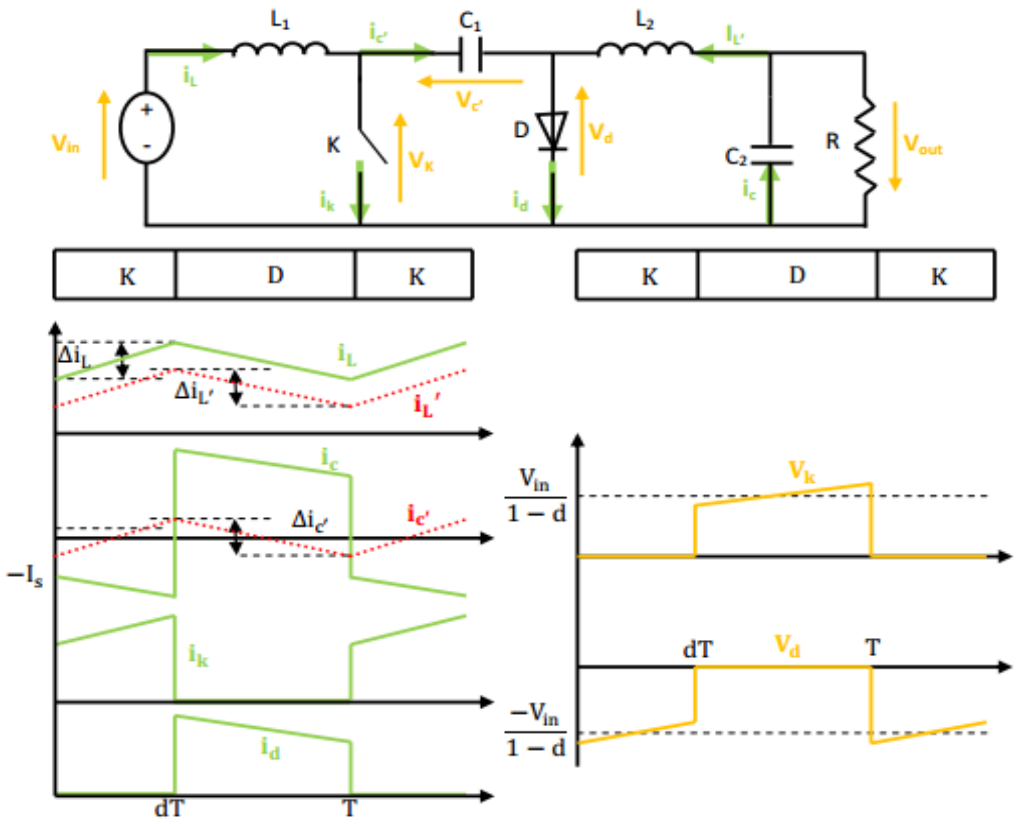

Fig. 1 Structure, currents and voltages of the cuk DC-DC converter

Thus, the modeling of the cuk converter can be expressed by multiplying (1) by d and (2) by $1-d$:

$$\begin{aligned}\frac{di_L}{dt} &= \frac{V_{in}}{L_1} - \frac{V_{C'}}{L_1}\cdot(1-d)\\ \frac{dv_{c'}}{dt} &= \frac{i_{L_1}}{C_1}\cdot(1-d) + \frac{i_{L'}}{C_1}\cdot d\\ \frac{di_{L'}}{dt} &= \frac{V_{out}}{L_2} - \frac{V_{c'}}{L_2}\cdot d\end{aligned} \quad (4)$$

The preceding expression fairly shows that the chopper is managed by nonlinear equations. The static gain in function of the duty cycle is given by:

$$V_{out} = \frac{d}{1-d}\cdot V_{in} \quad (5)$$

We remark that the static converter acts as a voltage booster for $d > 0.5$ and as a lowered voltage for $d < 0.5$.

Both inductors have current ripples of:

$$\Delta i_L = \frac{d\cdot V_{in}}{L_1\cdot f} \quad (6)$$

$$\Delta i_{L'} = \frac{d\cdot V_{in}}{L_2\cdot f} \quad (7)$$

The voltage ripple through R :

$$\Delta V_{out} = \frac{\Delta i_{L'}}{8 C_1 f} = \frac{d\cdot V_{in}}{8 L_2 C_1 f^2} \quad (8)$$

The voltage ripple through C_2

$$\Delta V_{C_2} = \frac{(1-d) I_L}{C_2 f} = \frac{d^2 V_{in}}{(1-d) R C_2 f} \quad (9)$$

The constraints on the switch k and the diode D are:

$$V_{K,max} = \left|V_{d,max}\right| = V_{c_2,max} = \frac{V_{in}}{1-d} + \frac{\Delta V_{c_2}}{2} \quad (10)$$

$$i_{K,max} = i_{d,max} = I_L + I_{L'} + \frac{\Delta i_L + \Delta i_{L'}}{2} \quad (11)$$

Table 1 provides the different parameters employed in simulation.

Table I. Main parameters of the solar PV system

P_{max}	59.85 W
V_{oc}	21.1 V
I_{sc}	3.8 A
V_{mpp}	17.1 V
I_{mpp}	3.5 A
k_v	-0.08 V/°C
k_i	0.003 A/°C
f	20kHz
L_1	5mH
L_2	5mH
C_1	47µF
C_2	1µF
R	10 Ω
V_b	12 V

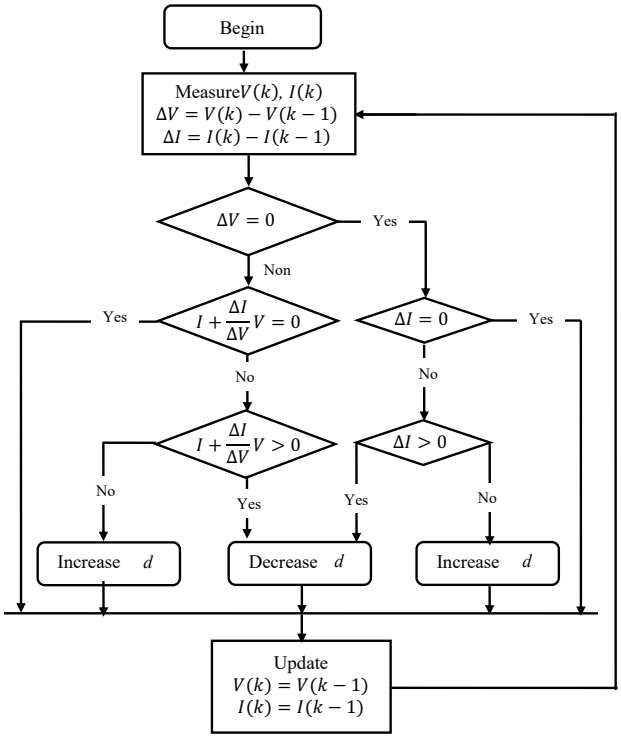

Fig. 2 Diagram of the direct duty cycle INC-MPPT algorithm

IV. DIRECT DUTY CYCLE INC MPPT

The INC MPPT method follows the MPP that is corresponds to the knee of the current vs. voltage curve or to the top of the power vs. voltage curve by comparing the instantaneous conductance to the negative of differential conductance [14-19]. The slope of the power vs. voltage curve ($\frac{dP}{dV} = I + \frac{\Delta I}{\Delta V} \cdot V$) reaches zero at the MPP, superior than zero on the left of it and inferior than zero on the right. The operating voltage must be decreased when the slope is negative and it must be increased when the slope is positive. Finally, when the MPP is reached, the slope of the P-V curve becomes zero and the control thus stops disturbing the photovoltaic voltage. Fig.2 shows the diagram that describes the working principle of this control algorithm. The ripple rate and the speed of tracking in which the algorithm follows the MPP depend on the disruption step of the duty cycle of the converter.

This method has two major handicaps which are: In established regime, the operating point never reaches the MPP but oscillates around. In dynamic regime when the illumination varies quickly, the algorithm can deviate from the MPP [17-18].

V. LEAD ACID BATTERY

An autonomous electrical system is chosen for locations where the public network is absent or remote from the installation site. It represents an independent energy source and serves to supply users with electricity without being connected to the electricity grid. This type of system is reliable and is protected against power cuts caused by weather problems or network failures. Generally, an autonomous system alone cannot satisfy the energy demand of the users. A storage medium is essential especially if the resources are intermittent, as in the case of a photovoltaic installation or a wind turbine. The electrical energy is stored indirectly via another form of energy except in special cases as capacitors or supercapacitors. It is therefore essential to transform electricity into storable energy. According to the International Energy Agency (IEA), 99% of electricity storage stations in the world is based on STEP, Pumped Energy Transfer Stations. There are other storage methods, such as flywheel storage, energy storage by compression of the air, hydrogen storage, capacitor/supercapacitor electrostatic energy storage, superconducting magnetic energy storage, electrochemical storage using batteries and so on. Batteries convert electrical energy into chemical energy and vice versa throughout charge/discharge cycles. A battery cell is composed of two plates submerged in an insulating material. Two oxidation-reduction half reactions occur between the plates and the insulating solution, producing the release of ions and electrons in the electrolytic solution, which means that an electrical current is established between the two electrodes. Three types of batteries exist depending on the area of application, starter batteries for cars, traction batteries for forklifts, and stationary batteries for uninterruptible power supplies. According to the used materials we can find several categories of battery like: Nickel-Cadmium, Nickel Metal Hydride, Lead-Acid, Lithium, Zinc-Air, Sodium-Sulfur, etc. Batteries with a low storage capacity ranging from a few Wh to a few tens of kWh are used for portable or integrated applications, but also for backup functions in systems connected to the network. However, some batteries such as Nickel-Cadmium, Lead-Acid, and Sodium-Sulfur have been utilized in numerous large scale storage systems.

Since the PV source is intermittent, an off-grid PV system has need of storage batteries. The state of charge (SoC) parameter is a significant quantity in a battery, is equal to the ratio of the present capacity to the capacity when the storage battery is fully charged. The SoC parameter takes values from 0% (battery fully discharged) to 100% (battery fully charged). The battery voltage parameter depends powerfully on the SoC factor.

Lead-acid battery having a nominal voltage of 12 volt is employed for non-interruptible power supplies in PV application. The charged battery is composed by lead cathode (Pb), a lead dioxide anode (PbO_2) and an insulating electrolyte formed of H_3O^+ and HSO_4^- [20]. The oxidation-

reduction reactions that describe the working principle of this battery are as follows:

Oxidation of Pb in $PbSO_4$

$$Pb + HSO_4^- + H_2O \underset{\text{charge}}{\overset{\text{discharge}}{\rightleftharpoons}} PbSO_4 + H_3O^+ + 2e^-$$

Reduction of PbO_2 in $PbSO_4$

$$PbO_2 + HSO_4^- + 3H_3O^+ + 2e^- \underset{\text{charge}}{\overset{\text{discharge}}{\rightleftharpoons}} PbSO_4 + 5H_2O$$

We add the two half-reactions to obtain the global oxidation-reduction reaction:

$$PbO_2 + 2H_2SO_4 + Pb \underset{\text{charge}}{\overset{\text{discharge}}{\rightleftharpoons}} 2PbSO_4 + H_2O$$

Lead acid battery [21-23] is reasonably priced; it requires little maintenance; no difficulty when charging; the riskiness of spontaneous discharge is small, permitting long-term storage; as well its recycling is simple. However, this type of battery is not immune to certain disadvantages such as: the risk of sulfating if the discharge level of the battery exceeds 80%; the energy/weight ratio is small between 7 and 20 Ah/kg; low life, 500 cycles; and the lead contaminates the environment at the end of life. Amongst the large scale electricity storage methods, it has been watched that lead acid batteries suitable for all applications have the cheapest cost after STEPs and compression air storage.

VI. RESULTS OF NUMERICAL SIMULATION

Fig. 3 depicts the scheme of the solar PV system. The cuk DC-DC converter with the direct duty cycle INC-MPPT technique is utilized to track the maximum power of the solar generator and to regulate the voltage levels between the PV source and the lead acid battery.
Numerical simulations were performed to illustrate the performance of the studied system under changing weather conditions. The effect of illumination on the behavior of the PV module is observed on the I-V and P-V characteristics of Fig. 4. It can be seen that the short-circuit current and the solar irradiance are linearly proportional but that the no-load voltage is just slightly affected by sunlight. Fig. 5 demonstrates by simulation the evolution of the curves of the PV maximum power, the true MPP, the optimal solar voltage, the charge voltage and the optimal solar current during a lighting change according to a trapezoidal profile. It can be observed that the optimal current effectively tracks the profile of the sunlight; the power attained is very close to the true MPP over the entire duration of the variation profile except for the start-up time; the comportment of the optimal voltage is just gently affected and the output voltage is reversed. The corresponding waveforms of the duty cycle and MPP tracking efficiency are described in Fig. 6. The average tracking efficiency corresponding to the change of irradiance is equal to 93.38 %.

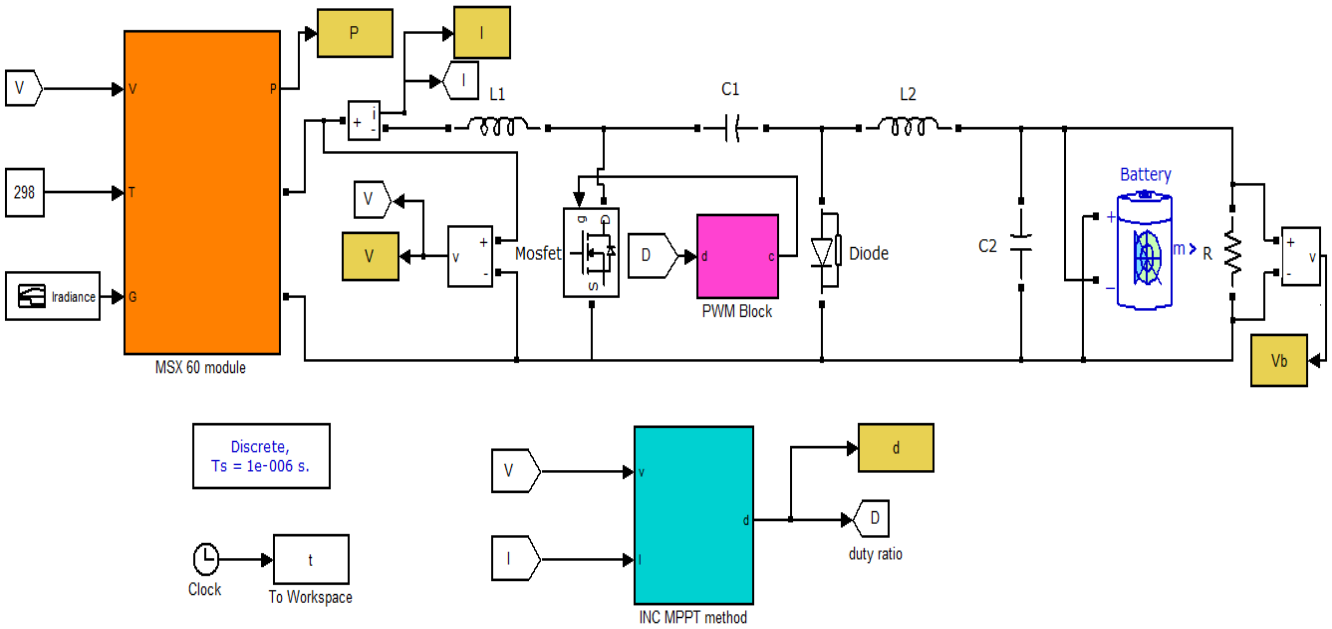

Fig. 3 The proposed PCU connecting the PV source and the battery

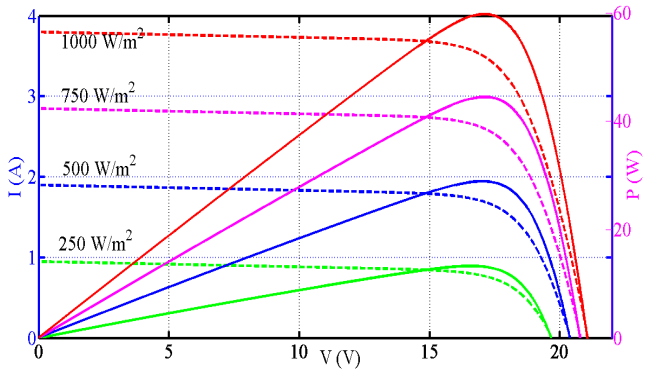

Fig. 4 Influence of illumination on PV characteristics

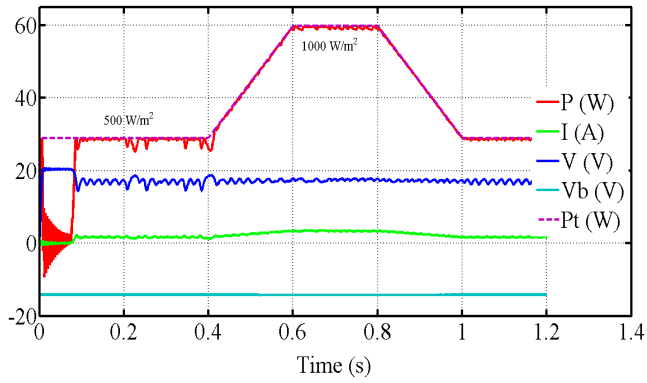

Fig. 5 PV maximum power, the true MPP, the optimal voltage, the battery voltage and the optimal current during a change of lighting

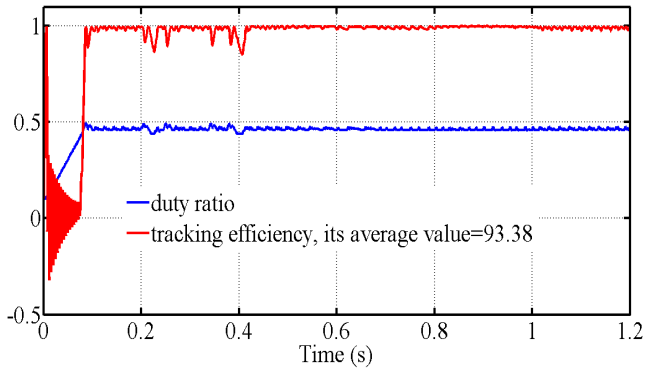

Fig. 6 Evolution of the duty cycle and the tracking effectiveness during a change of lighting

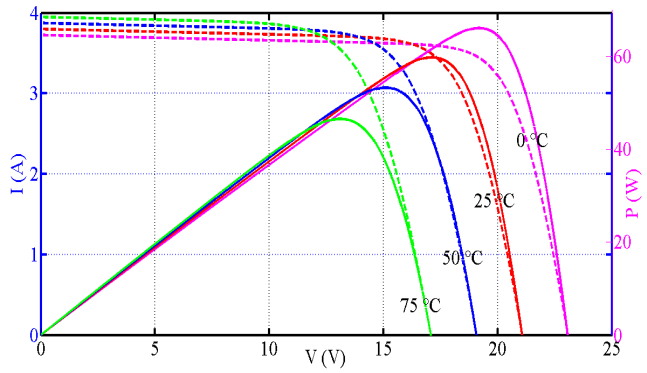

Fig. 7 Influence of temperature on PV characteristics

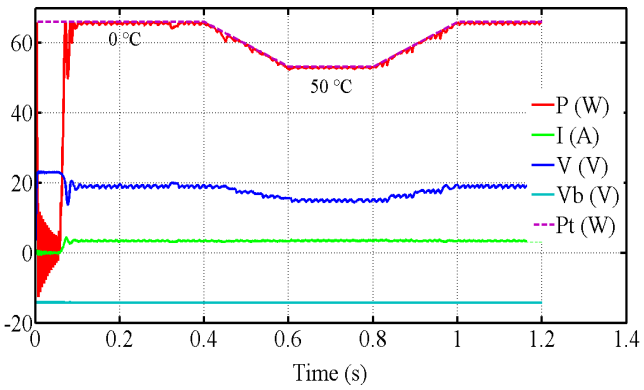

Fig. 8 PV maximum power, the true MPP, the optimal voltage, the battery voltage and the optimal current under a temperature change

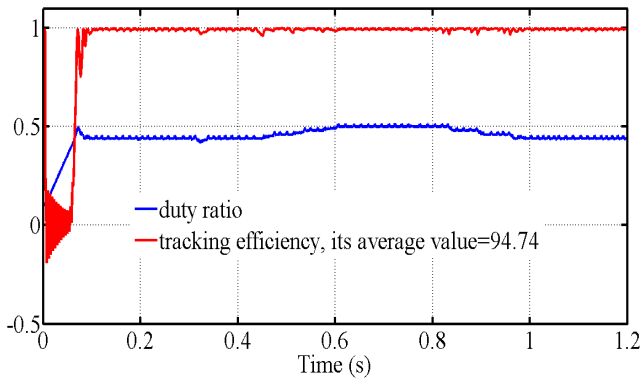

Fig. 9 Evolution of the duty cycle and the tracking effectiveness during a change of temperature

Temperature is the second parameter that has an impact on the behavior of solar panels. The impact of temperature on the characteristics of the solar module is clearly illustrated in Fig. 7. It is found that the temperature does not affect very much the short-circuit current but it has a great influence in reverse on the open circuit voltage. The waveforms simulated during a trapezoidal temperature change of the various electrical quantities of the system, such as the maximum power obtained, the maximum available power, the MPP voltage, the MPP current and the voltage at the battery terminals are summarized in fig. 8. It can be observed that the MPP voltage effectively follows the temperature profile; the maximum power obtained is very close to the actual MPP over the entire duration of the change profile, with the exception of the start-up time; the current at the MPP is approximately unchanged and the voltage across the battery is also reversed. The corresponding curves of the converter duty cycle and the tracking competence are both shown in Fig. 9. The average tracking efficiency for the change in temperature is increased to 94.74 %. At last, we would like to inform that the step size employed in the simulations was equal to 0.00087.

VII. CONCLUSIONS

This document presents a cuk DC-DC converter controlled by the direct duty cycle INC-MPPT technique to track the PV maximum power and to regulate the voltage levels between the MSX 60 PV module and the 12 V lead-acid battery. The peak power tracking system was modelled within Simulink and power systems tools, well-designed for

an UPS storage application and controlled using a suitable MPPT algorithm. The recommended peak power cuk converter is uncomplicated, consistent and gives high-class results in case of changing environmental conditions. Unfortunately, there is no practical support for this study at this time; this will be accomplished in the next work.

ACKNOWLEDGMENTS

This work, carried out at the Department of Electromechanics of the Faculty of Science and Technology of Bordj Bou Arreridj University, in Algeria, was supported by the CNEPRU research project No. **A01L07UN340120150001;** and by the Faculty of Engineering and Architecture of **Nisantasi University**, Istanbul, Turkey. This support is greatly appreciated.

REFERENCES

[1] A.I.M. Ali et al. Modified efficient perturb and observe maximum power point tracking technique for grid-tied PV system. Electrical Power and Energy Systems 99 (2018) 192–202.

[2] Tsai J-F, Chen Y-P, Sliding mode control and stability analysis of buck DC-DC converter. International Journal of Electronics, Vol. 94, No. 3, March 2007, 209–222.

[3] A. Hidaka, T Tsuji, S. Matsumoto, "A Thermoelectric Power Generation System with Ultra low Input Voltage Boost Converter with Maximum power Point Tracking", 1st International Conference on Renewable Energy Research and Applications (ICRERA), Milwakuee, USA 19-22 Oct 2012, pp. 1-5.

[4] Soon Tey Kok, Mekhilef Saad, Safari Azadeh. Simple and low cost incremental conductance maximum power point tracking using buck-boost converter. J Renew Sustain Energy 2013;5:023106.

[5] Ghassami A.A., Sadeghzadeh S.M., Soleimani A., (2013), A high performance maximum power point tracker for PV Systems, Electr. Power Energy Syst. 53, 237-243.

[6] Safari A, Mekhilef S. Simulation and hardware implementation of incremental conductance MPPT with direct control method using cuk converter. IEEE Trans Ind Electron 2011;58:1154–61.

[7] H. F. M. Lopez et al , "Analog signal processing for photovoltaic panels grid-tied by Zeta converter", 2009 IEEE Electrical Power & Energy Conference (EPEC), Milwakuee, USA 22-23 Oct 2009, pp. 1-6.

[8] Veerachary M. Power tracking for nonlinear PV sources with coupled inductor SEPIC converter. IEEE Trans Aerosp Electron Syst 2005;41:1019–29.

[9] Mohamed Azab., "DC power optimizer for PV modules using SEPIC converter", 2017 IEEE International Conference on Smart Energy Grid Engineering (SEGE), pp. 74-78.

[10] Poornima Mazumdar ; Prasad N. Enjeti ; Robert S. Balog, "Analysis and Design of Smart PV Modules," IEEE Journal of Emerging and Selected Topics in Power ElectronicsVolume: 2, Issue: 3 (2014) 451–459.

[11] Moumita Das ; Vivek Agarwal, "Novel High-Performance Stand-Alone Solar PV System With High-Gain High-Efficiency DC–DC Converter Power Stages", IEEE Transactions on Industry Applications, Volume: 51, Issue: 6 (2015) 4718–4728.

[12] Andreas Poullikkas. A comparative overview of large-scale battery systems for electricity storage. Renewable and Sustainable Energy Reviews 27 (2013) 778–788.

[13] Dileep. G, S.N. Singh. Selection of non-isolated DC-DC converters for solar photovoltaic system. Renewable and Sustainable Energy Reviews 76 (2017) 1230–1247.

[14] Xingshuo Li ; Huiqing Wen ; Yihua Hu "Evaluation of different maximum power point tracking (MPPT) techniques based on practical meteorological data", 5th International Conference on Renewable Energy Research and Applications (ICRERA), Birmingham, UK, 20-23 Nov 2016, pp. 696 - 701.

[15] S. Gautam, D. B. Raut, P. Neupane, D. P. Ghale, R. Dhakale "Maximum Power Point Tracker with solar prioritizer in Photovoltaic application", 5th International Conference on Renewable Energy Research and Applications (ICRERA), Birmingham, UK, 20-23 Nov 2016, pp. 1051-1054.

[16] Kok Soon Tey, SaadMekhilef. Modified incremental conductance MPPT algorithm to mitigate inaccurate responses under fast-changing solar irradiation level. Solar Energy, 2014; 101, p. 333-342.

[17] A.Belkaid, I.Colak, O.Isik, "Photovoltaic maximum power point tracking under fast varying of solar radiation", Applied Energy 179 (2016) 523–530, http://dx.doi.org/10.1016/j.apenergy.2016.07.034 .

[18] A.Belkaid, I.Colak, K. Kayisli, "A comprehensive study of different photovoltaic peak power tracking methods", 6th International Conference on Renewable Energy Research and Applications (ICRERA), San Diego, CA, 5-8 Nov 2017, pp. 1073 - 1079.

[19] K. Kumar, N. Ramesh Babu, K. R. Prabhu, "Design and Analysis of an Integrated Cuk-SEPIC Converter with MPPT for Standalone Wind/PV Hybrid System",Int. J. Renew. Energ. Res., vol. 7, N° 1, pp. 96-106, 2017.

[20] Hung-I Hsieh ; Sheng-Fang Shih; Jen-Hao Hsieh; Guan-Chyun Hsieh "A study of high-frequency photovoltaic pulse charger for lead-acid battery guided by PI-INC MPPT", International Conference on Renewable Energy Research and Applications (ICRERA), Nagasaki, Japan, 11-14 Nov 2012, pp. 1-6.

[21] M. Madaci, D. Kerdoun, "Conception optimization and CFD structure study of Wind firm power generation based on OWC-WTGS combined generation system with battery storage system", Int. J. Renew. Energ. Res., vol. 7, N° 2, pp. 496-512, 2017.

[22] Ali Q. Al-Shetwi, "Design and Economic Evaluation of Electrification of Small Villages in Rural Area in Yemen Using Stand-Alone PV System", Int. J. Renew. Energ. Res., vol. 6, N° 1, pp. 289-298, 2016.

[23] A. T. Mahamadou, B. C. Mamadou, D. Brayima, N. Cristian, "Ultracapacitors and Batteries integration for Power Fluctuations mitigation in Wind-PV-Diesel Hybrid System", Int. J. Renew. Energ. Res., vol. 1, N° 2, pp. 86-95, 2011.

[24] Mohammed H. Albadi, A. S. Al-Busaidi, E. F. El-Saadany, "Seawater PHES to Facilitate Wind Power Integration in Dry Coastal Areas – Duqm Case Study", Int. J. Renew. Energ. Res., vol. 7, N° 3, pp. 1363-1375, 2017.

[25] M. Moazzami, M. Ghanbari, J. Moradi, H. Shahinzadeh, G. B. Gharehpetian, "Probabilistic SCUC Considering Implication of Compressed Air Energy Storage on Redressing Intermittent Load and Stochastic Wind Generation", Int. J. Renew. Energ. Res., vol. 8, N° 2, pp. 767-783, 2018.